

Concept and Application of LPM—A Novel 3-D Local Position Measurement System

Andreas Stelzer, *Member, IEEE*, Klaus Pourvoyeur, and Alexander Fischer

Abstract—Precise measurement of the local position of moveable targets in three dimensions is still considered to be a challenge. With the presented local position measurement technology, a novel system, consisting of small and lightweight measurement transponders and a number of fixed base stations, is introduced. The system is operating in the 5.8-GHz industrial–scientific–medical band and can handle up to 1000 measurements per second with accuracies down to a few centimeters. Mathematical evaluation is based on a mechanical equivalent circuit. Measurement results obtained with prototype boards demonstrate the feasibility of the proposed technology in a practical application at a race track.

Index Terms—Frequency-modulated continuous wave (FMCW), global positioning system (GPS), local position measurement (LPM), three-dimensional (3-D) position estimation.

I. INTRODUCTION

NUMEROUS applications require the knowledge of the exact position of moving targets. With the global positioning system (GPS), there exists a widespread technology for global positioning with limited accuracy (without additional corrections) and measurement speed. For industrial tracking applications, it is often required to know the position of a target within a locally restricted area [1], [2]. The local position measurement (LPM) system fills this gap by providing the actual position of numerous targets in three dimensions with high accuracy and short measurement cycles [3], [4]. The LPM concept is, in some aspects, inverse to GPS as there are active transponders operating around 5.8 GHz, whose positions are measured, and as there are fixed passive base stations (BSs) around the covered field of view. The applications of LPM reach from the tracking of a single sportsman or a whole team in sports applications to the tracking of autonomous vehicles in industrial warehouses or the determination of the position of numerous vehicles and carts in operation on big airports.

In Sections II and III, the LPM concept and measurement principle are presented, followed by a novel mechanical equivalency for the mathematical problem on hand in Section IV. Hardware details are given in Section V and measurement results are presented in Section VI.

Manuscript received April 21, 2004; revised July 28, 2004. This work was supported in part by the Linz Center of Mechatronics (LCM) and by the Austrian Industrial Research Promotion Fund (FFF).

A. Stelzer is with the Institute for Communications and Information Engineering, Johannes Kepler University Linz, A-4040 Linz, Austria (e-mail: a.stelzer@icic.jku.at).

K. Pourvoyeur is with the Linz Center of Mechatronics GmbH, A-4040 Linz, Austria (e-mail: klaus.pourvoyeur@lcm.at).

A. Fischer is with Abatec Electronic AG, A-4844 Regau, Austria (e-mail: fischer@abatec.at).

Digital Object Identifier 10.1109/TMTT.2004.838281

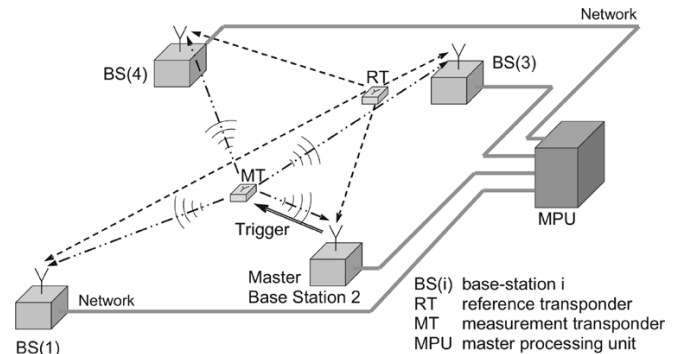


Fig. 1. Basic arrangement of transponders, BSs, and MPU, and the signal flow within the LPM system.

II. OVERVIEW OF THE LPM CONCEPT

The basic structure of the LPM system is sketched in Fig. 1. For simplicity, only one measurement transponder (MT) and four BSs are drawn. A master processing unit (MPU) is connected to the network and collects raw data for the final transponder position calculations.

At least four BSs are arranged on exactly known positions around the field of interest. The unknown position of the MT is determined by means of time-of-flight (TOF) measurements of electromagnetic waves traveling from the transponder to the BSs.

As the distances are short—the TOF is in the range of some hundreds of nanoseconds to microseconds—an evaluation in the frequency domain based on linear chirps is chosen. For TOF measurements, a common and highly accurate time base on the transponder and BSs would be necessary. To circumvent this, the time difference of arrival (TDOA) to different BSs is instead measured. Nevertheless, a synchronization of the BSs is required. As atomic clocks or high-speed optical fibers have to be ruled out due to cost reasons, the synchronization problem is solved by applying an additional low-cost transmitter, which serves as a reference transponder (RT) at a well-known and fixed position.

From an operational point-of-view, the reference transmitter operates continuously to keep the BSs synchronized, whereas the individual MTs are activated by means of a trigger telegram. For this reason, the BSs can also transmit control telegrams, but during the measurement cycle, they operate as receiver only. Furthermore, the transponder can send additional bytes of information to the BS, e.g., some measurement information captured by the mobile transponder.

During each measurement slot, only one MT is active. This time sharing guarantees that several MTs do not interfere with

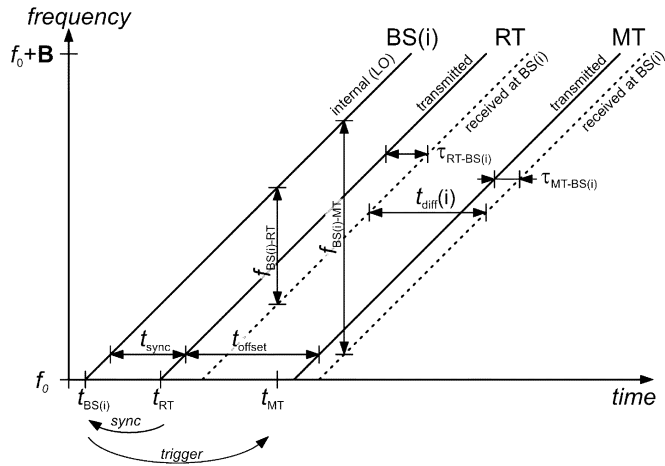


Fig. 2. Sketch of ramp signals in the LPM system with frequencies plotted versus time.

one another, moreover, the calculating time does not increase with the number of transponders.

III. MEASUREMENT PRINCIPLE

The basic concept of LPM relies on the well-known frequency-modulated continuous-wave (FMCW) radar [5] principle. In contrast to the FMCW principle, where the reflected and time shifted wave is mixed with a part of the transmitted signal, in LPM, the linear chirp received from the transponder is mixed in each BS with an independently generated chirp [6]. Furthermore, the reference chirp is simultaneously sent with the measurement chirp and used for synchronization purposes. A detailed insight is given by the signal diagram depicted in Fig. 2.

The RT continuously transmits reference chirps and each BS ($BS(i)$) internally generates linear chirps with an unknown time shift t_{sync} . After having received an activation command, the selected measurement transponder (MT) responds with a linear chirp at time t_{MT} . The time of flight τ between RT and $BS(i)$ and MT and $BS(i)$ can be written in terms of distances d as

$$\tau_{\text{RT-BS}(i)} = \frac{d_{\text{RT-BS}(i)}}{c_0} = \frac{\| \text{RT} - \text{BS}(i) \|}{c_0} \quad (1)$$

$$\tau_{\text{MT-BS}(i)} = \frac{d_{\text{MT-BS}(i)}}{c_0} = \frac{\| \text{MT} - \text{BS}(i) \|}{c_0} \quad (2)$$

where $\| \cdot \|$ denotes the Euclidian distance, and c_0 is the velocity of light. Mixing the received RT and MT signals with the internally generated chirp leads to the following IFs:

$$f_{\text{BS}(i)\text{-RT}} = K(t_{\text{RT}} - t_{\text{BS}(i)}) + K \frac{\| \text{RT} - \text{BS}(i) \|}{c_0} \quad (3)$$

$$f_{\text{BS}(i)\text{-MT}} = K(t_{\text{MT}} - t_{\text{BS}(i)}) + K \frac{\| \text{MT} - \text{BS}(i) \|}{c_0} \quad (4)$$

where K denotes the slope of the linear ramp—it is assumed that all chirps have an identical slope. Now, each BS can calculate the frequency difference

which leads, after a spectral evaluation, to a time difference t_{diff} of the corresponding signals in the time domain

$$c_0 t_{\text{diff}}(i) = c_0(t_{\text{MT}} - t_{\text{RT}}) + \| \text{MT} - \text{BS}(i) \| - \| \text{RT} - \text{BS}(i) \| . \quad (6)$$

Note that, t_{MT} and t_{RT} are unknown, but identical for all BS evaluations, resulting in a constant offset

$$t_{\text{offset}} = t_{\text{MT}} - t_{\text{RT}} . \quad (7)$$

IV. POSITION CALCULATION

A. Geometrical Illustration

Basically, LPM measures the time difference of electromagnetic waves traveling from different transponders to the BSs, containing an unknown offset t_{offset} in the raw data. Because of a known and constant propagation velocity of the electromagnetic wave, these time differences can be viewed as distances.

From a mathematical point-of-view, the position calculation in LPM is similar to the methods used in the GPS, as there are satellites with known positions and a receiver with an unknown position and a time offset due to a missing synchronization between the receiver and satellites. Therefore, the calculations for the dilution of precision (DOP) and all its derived quantities can be adapted from the mathematics used in the GPS [7]. This can be used to optimize the arrangement of BSs for the problem on hand. For the GPS, it is possible to track this offset, whereas in LPM, the unknown offset is not determined by the past offsets.

Due to the unknown offset, a measurement of a single BS contains no information about the position of the MT. Only a combined data set of several BSs allows us to compute the position of the MT, e.g., for three-dimensional (3-D) applications, the result of two BSs restricts the solution of the MT position to a hyperboloid. Hence, for 3-D applications, the measurement results of at least four BS are necessary to calculate the three unknown coordinates of the MT and the offset. In case of only four BSs, no statement on the consistency of the measurement set is possible. Statements about the absolute accuracy are only possible by using calibrated reference points.

Equation (6) describes the special case without measurement errors. This equation can be extended with an error-term $e(i)$ representing the measurement error at $BS(i)$ by

$$e(i) = \| \text{MT} - \text{BS}(i) \| - \| L(i) \| + c_0 t_{\text{offset}} \quad (8)$$

with $\| L(i) \|$ defined by

$$\| L(i) \| = \| \text{RT} - \text{BS}(i) \| + c_0 t_{\text{diff}}(i) . \quad (9)$$

In Fig. 3, (8) is illustrated geometrically with $t_{\text{offset}} < 0$. From a mathematical point-of-view, it is irrelevant whether the

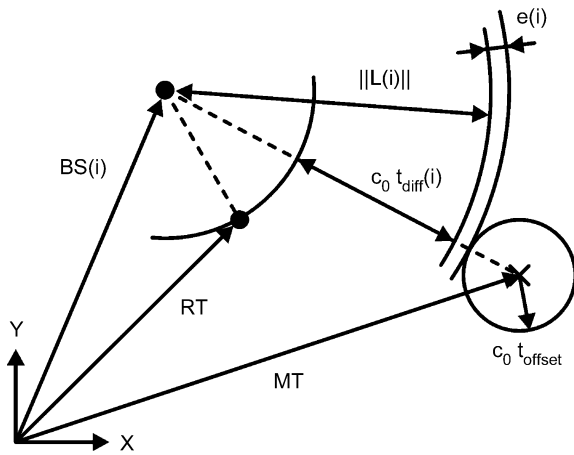


Fig. 3. Geometrical illustration of the LPM measurement principle in the 2-D case.

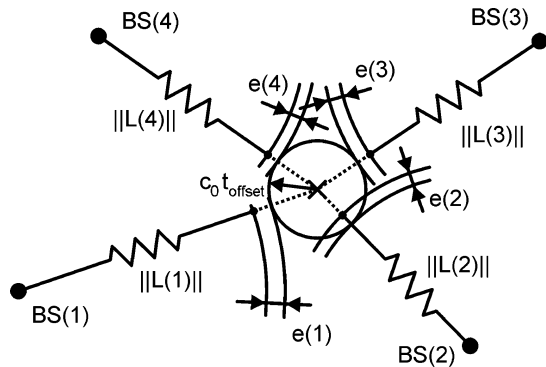


Fig. 4. Mechanical interpretation of the LPM measurement principle.

The position of the MT, and the measurement offset t_{offset} can be calculated, for example, by minimizing the weighted sum of the squared errors $e(i)$

$$\min J(\text{MT}, t_{\text{offset}}) = \min_{\text{MT}} \sum_{i=1}^N \gamma(i) e^2(i). \quad (10)$$

The weighting factor $\gamma(i)$ of the quality function J represents the measurement accuracy of BS(i), and N is the number of BSs available.

B. Mechanical Interpretation

It is possible to interpret the measurement principle of LPM in a mechanical sense. The variable $\|L(i)\|$ corresponds to the length of the spring i . The weight representing the measurement accuracy corresponds to the spring stiffness $k(i)$. The error $e(i)$ of BS(i) corresponds to the expansion of the spring i . Fig. 4 sketches the mechanical interpretation of the measurement principle for LPM.

The potential energy E_{pot} of all springs, representing the total energy of the mechanical system, is calculated as a sum of the potential energy $E_{\text{pot}}(i)$ of each individual spring i as follows:

The rest position of the mechanical system is given by a minimum of the total potential energy E_{pot} depending on the object position MT and the unknown offset t_{offset}

$$\min E_{\text{pot}}(\text{MT}, t_{\text{offset}}). \quad (12)$$

Amazingly, for

$$\gamma(i) = \frac{1}{2} k(i) \quad (13)$$

the two optimization problems (10) and (12) are identical. Based on the minimum of the total potential energy, it is possible to evaluate a mean error e_{mean}

$$e_{\text{mean}} = \sqrt{\frac{2}{k_{\text{mean}}} \min E_{\text{pot}}(\text{MT}, t_{\text{offset}})} \quad (14)$$

of the measurement set with

$$k_{\text{mean}} = \frac{1}{N} \sum_{i=1}^N k(i). \quad (15)$$

This mean error e_{mean} describes the consistency of the measurement set, it does not state anything about the absolute accuracy of the determined position.

As a first approximation, the estimated object position can be distinguished as Gauss distributed. In this case, the variance σ_{xy} of the estimated object position can directly be estimated by the mean error e_{mean} as follows:

$$\sigma_{xy} \cong e_{\text{mean}}. \quad (16)$$

Additional information about the accuracy of the estimated position is of enormous importance to improve the performance of tracking filters.

C. Solver

During the last three centuries, mechanical engineers such as Euler, Lagrange, and others developed powerful methods to derive differential equations for mechanical systems and especially to determine the rest position of these systems. The mechanical interpretation of the LPM measurement principle gives us the ability to use these highly advanced methods directly [8].

Hence, to solve the minimization problem of (12), we used a multidimensional damped Newton iteration for nonlinear regression [9], which was specially adapted to fit the demands of mechanical problems.

The nonlinear and, in the general case, redundant optimization problem could also be solved, for example, by using advanced filter concepts [10]. The potential of the applied specially adapted multidimensional damped Newton iteration method for different starting points is shown in Fig. 5 based on a real BS arrangement and synthetic measurement data without measurement errors. Plotted are the target position (marked with a filled square), the position of a BS used for position detection (marked with a filled circle), and the position of a

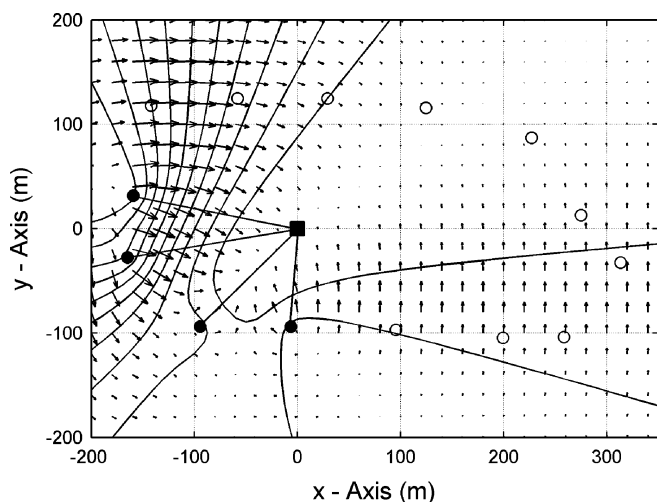


Fig. 5. Ways of iteration for a damped Newton iteration method for different starting points.

The quality function defined by the weighted sum of the squared errors can be interpreted as a potential field, its contour lines are visualized by solid lines. The gradient of the quality function is a vector valued function. For each point in the two-dimensional (2-D) plane, the direction of the arrows shows the direction of the gradient for this possible position of the MT, the lengths of these arrows correspond to the absolute value of the gradient. The measurement offset t_{offset} was calculated iteratively for each point in the plot. The rough positions of the available BS are chosen as starting points of the iteration. The ways of iteration are displayed by solid lines. As can be seen, the signals of four uneven distributed BSs were used to determine the position of the MT. This uneven distribution of the position of the BS around the target leads to a breaking up of the quality function on the opposite side of the BS. Such a BS distribution shows a worst case scenario; the breaking up effect can be suppressed by choosing the BS more uniformly distributed around the MT. In the breaking-up area, the gradient becomes very small. As can be seen, our specially adapted multidimensional damped Newton iteration method can handle these small gradients almost perfectly. Within a very few number of iteration steps, the solution of the optimization problem has been found. Even the choice of the starting point of the iteration is uncritical.

V. LPM HARDWARE

In Fig. 6, the block diagram of the transponder is shown. The receive path with a low-noise amplifier (LNA) for the reception of the activation command sent by the actual master BS is sketched in the upper half of the block diagram. The RF paths are separated by a switch. When activated, a measurement chirp is generated by the chirp generator, amplified by the power amplifier (PA), and finally transmitted via the antenna.

Fig. 7 shows the small and lightweight transponder printed circuit board (PCB).

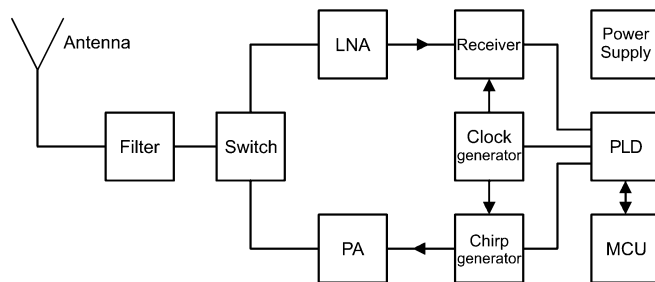


Fig. 6. Block diagram of a transponder in the LPM system.

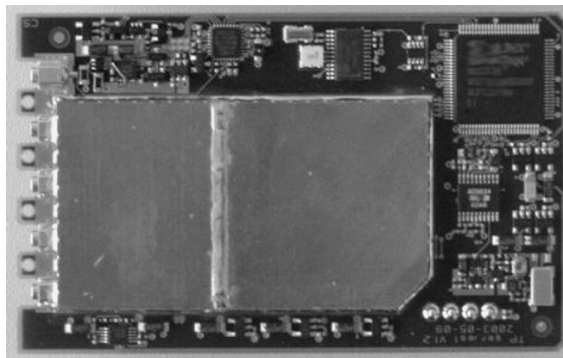


Fig. 7. Transponder PCB.

A power supply, programmable logic device (PLD), master control unit (MCU), and clock and chirp generator are common to both devices.

In the BS, which works as a receiver during the measurement cycle, the measurement chirp transmitted by the transponder is mixed with an internally generated chirp. Coherent mixing of these signals demands extremely high linearity of the generated chirps [6]. The digitized IF signal is pre-evaluated using a digital signal processor (DSP) and preprocessed data is transmitted to the MPU via the network.

In the current development state, the transponder hardware is as small as a credit card and weighs approximately 75 g. The BSs are slightly larger, but fit into approximately 1 dm³ and are generally mounted on masts around the field of view.

VI. MEASUREMENT RESULTS

The motor sports center at the Wachau Race Track, Melk, Austria, has been equipped with a prototype LPM system. An aerial view is shown in Fig. 8. The LPM control unit was installed at the paddock club above the pit lane.

The measurement accuracy was tested with a transponder mounted on a precision rail. The results obtained show a position error in the range of few centimeters at measurement rates of up to 1000 per second. The coverage of a single measurement cell is up to 500 m × 500 m. Larger areas can be monitored by combining basic measurement cells.

A more illustrative example is tracking of a car on an infield lap on the race track, as shown in Fig. 9.

The solid line visualizes the trajectory of the car in the 2-D plane, a filled circle marks the position of a BS. The start and



Fig. 8. Aerial view of the Wachau Race Track (reprinted with permission of the Austrian automobile club ÖAMTC).

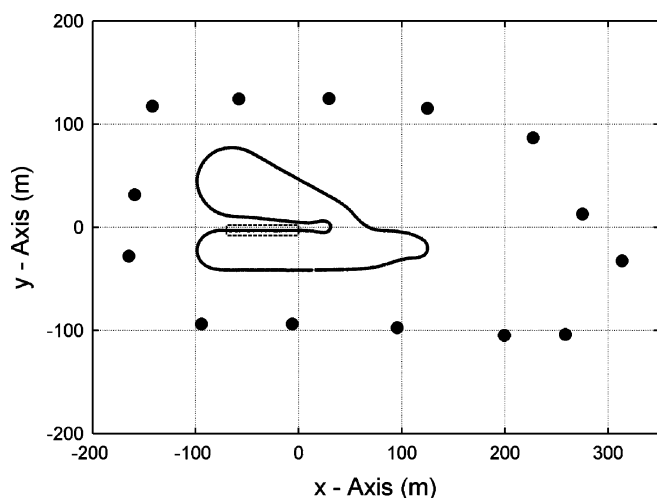


Fig. 9. Measured position data of a car on an infield lap on the Wachau Race Track.

car was approximately 80 km/h. The area surrounded by dashed lines is shown in detail in Fig. 10.

As we can see, almost all estimated positions are in a tube of ± 10 cm, visualized by dashed lines. These results were achieved without any tracking. Fig. 11 shows the corresponding total potential energy. To improve the comparableness to Fig. 10, the abscissa was scaled in x -coordinates of the object and not in samples, as it would be the nature of this signal.

As we can see, the total potential energy increases clearly around $x = -67$ m and $x = -48$ m. These increases are directly related to prongs of the estimated y -coordinate of the object position.

By using $g-h$, $g-h-k$, or Kalman filters for object tracking [11], the precision of the position detection can be increased clearly. Another advantage of such filters would be an estimation of the velocity and the acceleration of the target. To achieve an adequate performance of such tracking filters, the approximate knowledge of the accuracy of the estimated position is needed. By using (14) and (16), the total potential energy can be directly converted into the variance σ_{xy} of the object position.

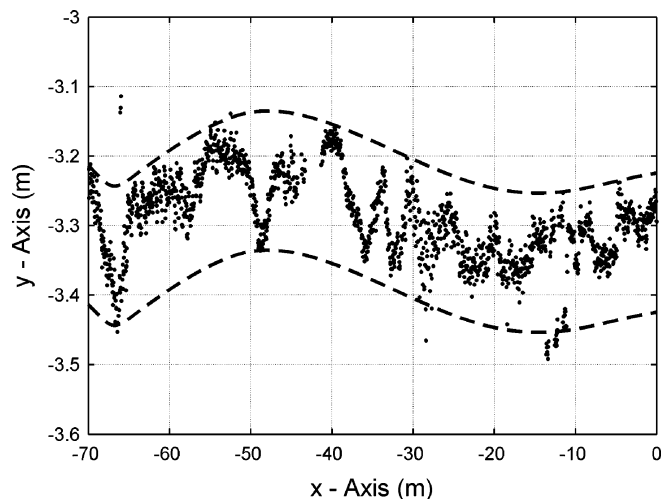


Fig. 10. Detailed view of a section for the infield lap on the Wachau Race Track.

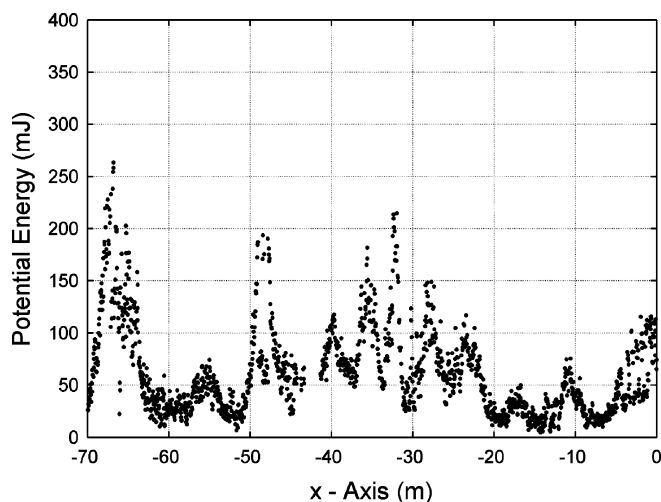


Fig. 11. Total potential energy of the spring-based model for position evaluation with abscissa scaled in x -coordinates of the object.

ample, time differences of two cars are now available for every point in time and are no longer restricted to the end of certain sectors.

VII. CONCLUSION

With local position measurements, a novel technology for fast and accurate LPMs is available. The LPM system operates within a license-free industrial–scientific–medical (ISM) band and the current design is compliant to European regulations.

Within a covered range of 500 m in square, the accuracy is better than 10 cm, depending on multipath and line-of-sight connections. Applications spread from analyzing movements in sports over industrial positioning to autonomous vehicle and cart control.

REFERENCES

- [11] M. Vossiek, L. Wiebking, P. Gulden, J. Wieghardt, and C. Hoffmann.

Explore Litigation Insights

Docket Alarm provides insights to develop a more informed litigation strategy and the peace of mind of knowing you're on top of things.

Real-Time Litigation Alerts



Keep your litigation team up-to-date with **real-time alerts** and advanced team management tools built for the enterprise, all while greatly reducing PACER spend.

Our comprehensive service means we can handle Federal, State, and Administrative courts across the country.

Advanced Docket Research



With over 230 million records, Docket Alarm's cloud-native docket research platform finds what other services can't. Coverage includes Federal, State, plus PTAB, TTAB, ITC and NLRB decisions, all in one place.

Identify arguments that have been successful in the past with full text, pinpoint searching. Link to case law cited within any court document via Fastcase.

Analytics At Your Fingertips



Learn what happened the last time a particular judge, opposing counsel or company faced cases similar to yours.

Advanced out-of-the-box PTAB and TTAB analytics are always at your fingertips.

API

Docket Alarm offers a powerful API (application programming interface) to developers that want to integrate case filings into their apps.

LAW FIRMS

Build custom dashboards for your attorneys and clients with live data direct from the court.

Automate many repetitive legal tasks like conflict checks, document management, and marketing.

FINANCIAL INSTITUTIONS

Litigation and bankruptcy checks for companies and debtors.

E-DISCOVERY AND LEGAL VENDORS

Sync your system to PACER to automate legal marketing.